Molecularly imprinted biomimetic SPR sensor decorated with gold nanoparticles for selective and sensitive detection of bisphenol A

ILGIM GÖKTÜRK , FATMA YILMAZ , Süleyman Aşır , DENİZ TÜRKMEN , Adil Denizli *

Posted Date: 19 December 2023

doi: 10.20944/preprints202312.1431.v1

Keywords: molecular imprinting; Bisfenol A; gold nanoparticles; surface plasmon resonance

Article

Molecularly Imprinted Biomimetic SPR Sensor Decorated with Gold Nanoparticles for Selective and Sensitive Detection of Bisphenol A

Ilgım Göktürk [1], Fatma Yılmaz [2], Süleyman Aşır [3,4], Deniz Türkmen [1] and Adil Denizli [1,*]

[1] Hacettepe University, Department of Chemistry, Beytepe, Ankara, Turkey; ilgim@hacettepe.edu.tr, denizt@hacettepe.edu.tr, denizli@hacettepe.edu.tr
[2] Bolu Abant Izzet Baysal University, Chemistry Technology Division, Gerede, Bolu, Turkey; yilmaz_f@ibu.edu.tr
[3] Near East University, Department of Biomedical Engineering, 99138, Nicosia, North Cyprus, Mersin 10, Turkey
[4] Near East University, Center for Science Technology and Engineering, 99138, Nicosia, North Cyprus, Mersin 10, Turkey; suleyman.asir@neu.edu.tr
* Correspondence: denizli@hacettepe.edu.tr

Abstract: MIPs inspired by antigen-antibody interactions have received substantial interest as a biomimetic artificial receptor system in environmental applications. Herein, we present a molecularly imprinted surface plasmon resonance (SPR) sensor integrated with Au nanoparticles for the identification of bisphenol A (BPA), an endocrine-disrupting chemical. We synthesized BPA-imprinted nanofilm consisting of amino acid-based functional monomers to detect selectively BPA from synthetic wastewater sample. The synthetic wastewater samples were analyzed to ensure the method's reliability and feasibility. Under ideal conditions, the suggested approach performed well in terms of analytical performance to BPA, with a wide linear range of 0.1 to 10 ppb and LOD of 10 ng/L. The sensor results and the Langmuir adsorption model have good agreement. It has also been shown that repeated use of the biosensor can be achieved. According to selectivity studies, BPA adsorbed within the imprinted cavities favorably compared to 4-nitrophenol and phenol. The produced BPA-imprinted SPR sensor provides improved sensitivity based on the signal amplification strategy, unconjugated sensing without the need for labeling, real-time sensing, low sample consumption rates, quantifiable assessment, and very good kinetic rate constant calculation in actual samples. Also, because the produced sensor is reusable with relative standard deviations (RSD)<1.25, indicating the sensor's accuracy, the SPR-based biomimetic BPA sensor is simple to practice and a cost-effective option.

Keywords: molecular imprinting; bisphenol A; gold nanoparticles; surface plasmon resonance

1. Introduction

The global concern for the impact of environmental pollutants on public health has sparked widespread attention and prompted numerous research endeavors. The essential task of separating and eliminating environmental contaminants is vital in mitigating the health risks posed to humans. Endocrine disruptors are substances that imitate or interfere with the body's hormones and can be found in the environment, food, personal care items, and fabricated goods. EDs can lead to a variety of issues in the human body, such as reproductive issues, immunological and neurological system dysfunction, and developmental abnormalities. Numerous items that we use daily include these compounds, including plastic storage receptacles, tinplate containers, cleansers, fire-resistant additives, nutrient products, toys, beauty products, insecticides, and herbicides. They pose a constant hazard to the human body as a result. Bisphenol A (BPA), hormones and their analogs are a couple of the most well-known examples.

 doi:10.20944/preprints202312.1431.v1

BPA is a chemical used mainly as a monomer in the manufacture of polymers. Additionally, it can be utilized as an inhibition agent for the polymerization of polyvinyl chloride or as an antioxidant in certain plasticizers [1,2]. Numerous materials used in the manufacture of children's items and food packaging contain BPA. BPA will inevitably be present in the environment due to the widespread use of plastics and the scale at which it is produced. It is quite toxic. The vast majority of individuals know about BPA as an endocrine disruptor [2–4]. Being exposed to BPA throughout the perinatal period may affect the development of the breast and prostate glands, resulting in alterations in brain biochemical communication in many potentially important brain areas and producing anxiety. Numerous studies have suggested that BPA has an impact on neural regeneration, genetic activity, the neurohormonal system, and the architecture of specific brain areas [5]. The potential for BPA to cause gene mutation and oncogenesis has also been demonstrated [6]. Due to BPA's high toxicity, the European Union prohibited its usage in the manufacture of polycarbonate infant bottles in 2011 [2]. Hormones can interfere with the endocrine system's ability to carry out physiological activities including development, growth, and reproduction, which makes their presence in the environment and diet a serious concern [7]. Hormone detection is crucial and necessitates a low LOD since any slight alteration in the organism's hormone levels might result in issues [8].

There is an increasing need for accurate and sensitive techniques to identify and measure BPA in various matrices due to the possible negative effects of BPA exposure. It is essential to detect BPA at trace levels in order to evaluate human exposure and guarantee regulatory compliance. In order to overcome the difficulties associated with BPA detection, scientists and researchers have created a variety of analytical techniques over time, each having specific benefits and drawbacks. There is a wide range of BPA detection methods, covering traditional techniques such as chromatography and spectrometry [9–11], as well as emerging technologies such as biosensors [12–15] and molecular imprinting [16,17]. According to studies based on the use of molecularly imprinted polymers (MIPs) for the detection, which has been the subject of several papers, BPA represents a large category of EDs [18–22]. Molecular imprinting technique, which has lately attracted a lot of interest, is being used to generate artificial materials that resemble antibodies and have recognition sites that have been properly prepared for recognizing the target molecule. Due to their great stability, excellent selectivity, and low cost, MIPs are thought to be a potential material for use as recognition elements for molecules [23–28]. The applications of SPR biosensors, which are characterized by rapid response, reliability and high performance, and have tremendous potential for label-free, real-time monitoring of various biomolecular interactions, have attracted great attention in recent years [29–38].

In this work, a molecularly imprinted SPR sensor system based on gold nanoparticles to increase sensitivity was effectively used to conduct sensitive and specific BPA detection in an aqueous solution. Amino acid-based functional monomers were used to fabricate the SPR biomimetic sensors. Briefly, gold nanoparticles were coordinated with N-methacryloyl-(L)-cysteine methyl ester (MAC) monomer, then BPA was complexed with N-methacryloyl-(L)-phenylalanine methyl ester (MAPA) monomer for the imprinting process. In order to preferentially detect target BPA molecules in the presence of competitor molecules, 4-nitrophenol and phenol, the selectivity investigation of gold nanoparticles decorated BPA-imprinted (MIP-Au) sensor was conducted. The efficacy of the imprinting procedure was assessed by contrasting the signal responses of the MIP-Au sensor and the NIP-Au sensor which was decorated with gold nanoparticles but non-imprinted. In this study, it was aimed to determine toxic BPA molecules using the molecular imprinting technique by the surface plasmon resonance sensor which allows direct, real-time, label-free, and quantitative detection of interactions by measuring refractive index change at or near a thin metal film surface.

2. Materials and Methods

Gold nanoparticles (40 nm in diameter) were purchased from SPI Supplies Inc (West Chester, PA, USA). The following substances were bought from Sigma (Chemical Co., ABD): 2-hydroxyethyl methacrylate, azoisobisbutyronitrile (AIBN), ethylene glycol dimethacrylate, BPA, 4-nitrophenol, and phenol. In Orsay, France, Genoptics sold us SPR chips (SPR-1000-050 SPR CHIP GWC). The experiments were carried out using an SPR imager II from GWC Technologies in Wisconsin, USA.

 doi:10.20944/preprints202312.1431.v1

2.1. Preparation of functional monomers

Functinol monomers (MAC and MAPA) were synthesized according to our previously published article [39]. Briefly, a mixture of 5.0 grams of phenylalanine or cysteine and 0.2 grams of sodium nitrite is dissolved in 30 ml of 5% (w/v) potassium carbonate. This mixture is then placed into a three-necked 100 ml distillation funnel. The reaction was magnetically stirred under nitrogen gas and allowed to cool in an ice bath at 0°C. Upon the reaction, 6 ml of methacryloyl chloride solution is added dropwise. The mixture taken from the ice bath is then mixed with a magnetic stirrer at RT for 2 hours. After this process, the pH of the mixture is adjusted and the pH is brought to 3:0. The resulting product is extracted in 50 ml of chloroform solution. Following the separation of the phases, the organic phase is dried with magnesium sulfate ($MgSO_4$), while the chloroform solution is evaporated in the evaporator. Then the functional monomers are finally crystallized and ready to use.

2.2. Preparation and characterization of biomimetic SPR sensors

A piranha solution with a ratio of 3 parts H_2SO_4 to 1 part H_2O_2 (v/v) was employed to meticulously clean the SPR chip. The cleaning process involved immersing the chip in 20 mL of the piranha solution for 30 seconds, followed by immersion in pure ethyl alcohol. After the chip was dried at room temperature, the SPR chip underwent surface modification utilizing allyl mercaptane to incorporate the vinyl groups. In summary, a 3.0 M solution of allyl mercaptane was prepared in an ethanol/water mixture (4:1, v/v). The SPR chip was immersed in this solution for a duration of 12 hours. Following the surface modification process, the chip underwent a thorough rinsing with ethanol and was subsequently dried under a nitrogen stream at room temperature.

MAC was mixed with AuNPs (0.01 nmol:0.01 mmol) for the coordination of AuNPs with MAC functional monomer. In order to create the MAPA-BPA pre-complex, 0.1 mmol MAPA and BPA in a 1:1 mole ratio were also combined for 30 min. The pre-complexed mixture was mixed with monomer solutions of 2-hydroxyethyl methacrylate (0.01 mmol) and ethylene glycol dimethacrylate (0.04 mmol). After the mixture had been agitated by the vortex for a while and AIBN (2 mg) had been added into the mixture, it (10 μL) was put over the SPR chip to prepare BPA-imprinted MIP-Au sensor. The polymerization reaction was started by exposing UV radiation on the chip's surface. After the polymerization was finished, 0.5 mM NaOH was used as a desorption agent to remove the template molecule BPA from the polymeric nanofilm. The same method was used to create the non-imprinted NIP-Au sensor, but BPA was not added as the target molecule. The same process was used to synthesize BPA-imprinted MIP sensor as well, but without the inclusion of AuNPs. For the purpose of characterizing SPR sensors, atomic force microscopy (AFM, Nanomagnetics Instruments, Oxford, England) and measurements of the contact angles with Kruss DSA100 (Hamburg, Germany) were conducted.

2.3. Kinetic analyzes of biomimetic SPR sensors

Kinetic studies were examined to evaluate the interactions between BPA-imprinted MIP-Au sensor and BPA molecules. Various concentrations of BPA were introduced into synthetic wastewater samples, which were subsequently utilized in the SPR system. The experimental procedure can be summarized as follows: initially, the SPR chip was washed with a 0.5 mM NaOH solution (10 mL, flow rate of 0.2 mL/min), followed by a subsequent wash with deionized water (20 mL, flow rate of 0.2 mL/min). Surface plasmon curves were derived, and the resonance angle was computed during the circulation of the equilibrium buffer. Subsequently, the mirror system was set up at the determined resonance angle, and kinetic studies were conducted at this specific angle to acquire surface plasmon resonance curves. The plasmon curve values were assessed and graphed as the angle of incident light versus the percentage of diffraction. For kinetic analysis studies, the SPR software served as the kinetic monitoring program. To establish a stable baseline, the equilibrium buffer was circulated, and subsequently, the BPA sample was introduced into the SPR system. The reflectivity (%) changes in resonance frequency occurred promptly upon the arrival of the BPA

Preprints (www.preprints.org) | NOT PEER-REVIEWED | Posted: 19 December 2023 doi:10.20944/preprints202312.1431.v1

solution at the SPR chip. The process of adsorption, desorption, and washing was iteratively carried out for each analysis. Kinetic studies were conducted to establish a linear range for the SPR chip, facilitating the determination of BPA in synthetic wastewater. The kinetic evaluations of MIP-Au, NIP-Au, and MIP sensors were performed using SPR imager II. To acclimate the sensors, an ethanol solution (%50 v/v) was run into the SPR apparatus with a 0.2 mL/min flow rate. The sensor system was then exposed to successive applications of BPA solutions with varying BPA concentrations ranging from 0.1 to 10 ppb. Each sample's variations in reflectance values served as a record of plasmonic responses. After attaining equilibrium, the target BPA molecule was desorbed off the surface of the sensors using a 0.5 mM NaOH solution flowing at the same rate.

2.4. Selectivity and imprinting efficiency

For selectivity investigations, 4-nitrophenol and phenol were chosen as competing reagents since the BPA molecule's structure and size are quite similar to theirs. Ten parts per billion of BPA and ten parts per billion of competitor molecules (4-nitrophenol and phenol solutions) were used in the adsorption tests for BPA detection. The competing compounds underwent the same kinetic analysis procedure. The difference between the signal responses of MIP-Au and NIP-Au sensors was used to calculate imprinting efficiency. By administering 10 ppb BPA solution in ethanol solution (%50 v/v) to both MIP-Au and NIP-Au sensors, the signal responses were obtained. MIP-Au and NIP-Au sensors were used for BPA adsorption and desorption tests. Equation (1) was used to construct an imprinting factor using the percent refractive change value (ΔR) to assess the imprinting efficiency.

$$\text{Imprinting factor} = \Delta R_{\text{MIP-Au sensor}} / \Delta R_{\text{NIP-Au sensor}} \quad (1)$$

2.5. Reusability and repeatability study

With their reusable features, molecularly imprinted SPR sensors are resistant to harsh environmental conditions with their stable polymeric structure. The reusability of MIP-Au sensor for the same BPA solution applied four times consecutively was tested. Repeatability tests of the MIP-Au sensors underwent statistical analysis using 10 ppb BPA for intraday testing (four duplicates in triplicate), and repeatability accuracy has been confirmed by determining the percent relative standard deviation (%RSD). Findings from intraday testing with %RSD reported were below 1.25, showing strong repeatability.

3. Results and Discussion

3.1. Characterization of biomimetic SPR sensors

The surface morphology of MIP-Au and NIP-Au sensors was investigated by AFM in a half-contact mode. After the imprinting process, the surface depth of the NIP-Au sensor was increased from 11.8 ±1.32 nm to 21.1±1.07 nm as shown in Figure 1. The imprinting procedure was accomplished effectively during the polymerization phase by comparing the surface depth values of NIP-Au and MIP-Au sensors.

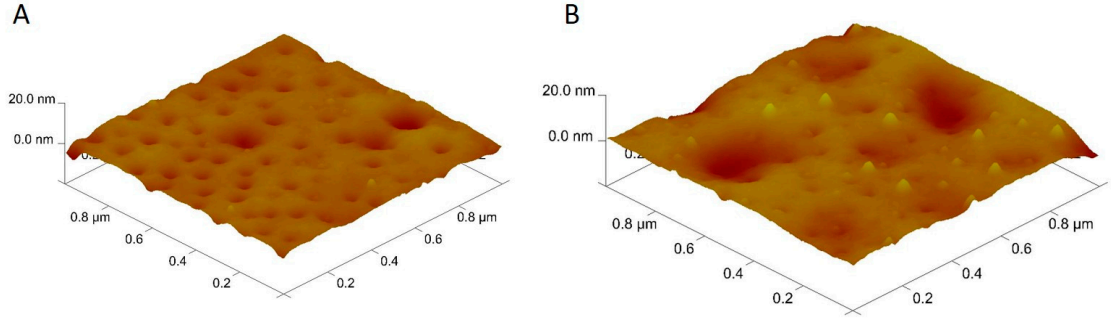

Figure 1. AFM images of A. NIP-Au and B. MIP-Au SPR sensors.

Preprints (www.preprints.org) | NOT PEER-REVIEWED | Posted: 19 December 2023 doi:10.20944/preprints202312.1431.v1

A contact angle instrument was used to measure the surface wettability of MIP-Au and NIP-Au SPR sensors, and DSA2 software was utilized to derive contact angle data. The contact angle pictures of the MIP-Au and NIP-Au sensors can be seen in Figure 2. The NIP-Au sensor's surface was measured to have a contact angle of 67.6°±1.6, whereas the MIP-Au sensor's contact angle was 71.2°±0.8. As determined by the contact angle measurements, it was found that the contact angle value increased after BPA imprinting, possibly as a result of a decrease in surface wettability following the coordination of the BPA molecule with the functional MAPA monomer.

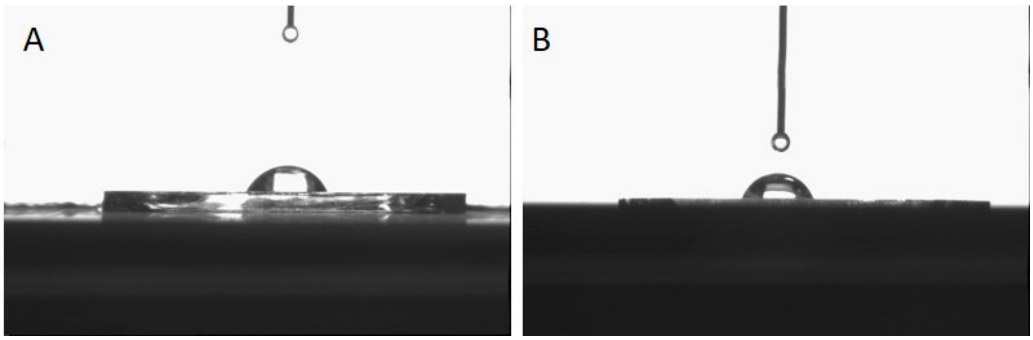

Figure 2. Contact angle measurements of sensors A) MIP-Au, B) NIP-Au SPR sensor.

3.2. Kinetic analyzes of biomimetic SPR sensors

Kinetic studies were conducted to examine the adsorption dynamics and characteristics of BPA detection. For that, real-time monitoring of the BPA attachment from ethanol solution (%50 v/v) on the molecularly imprinted SPR chip surface was carried out using the BPA-imprinted MIP-Au SPR sensor. Different concentrations of BPA in ethanol solution, ranging from 0.1 to 10 ppb, were tested on the MIP-Au sensor. The recorded % change in the surface plasmon resonance angle (ΔR) was used to determine the adsorption dynamics. Figure 3A shows the whole process performed for the BPA detection, including equilibration, adsorption, desorption, and regeneration, which were nearly finished in seven minutes. As deduced from the graph, the sensor response increased as BPA levels increased.

The MIP-Au sensor's equilibrium and kinetic isotherm parameters were determined via Equations (2–6). If the overall amount of binding region can be described by means of the highest analyte binding capability of the chip's surface, the entire concentration parameters are then able to be defined in terms of the SPR response signal ΔR, negating the necessity for conversion from mass to molar concentrations. The binding is characterized by equation (2) under pseudo-first-order conditions, where the concentration of free analyte in the flow cell is maintained constant. Four distinct equilibrium isotherm models—Scatchard, Langmuir, Freundlich, and Langmuir-Freundlich—were analyzed for equilibrium data in order to define the interaction model between the BPA imprinted MIP-Au SPR sensor and BPA molecules.

$$\text{Equilibrium kinetic analysis } \frac{d\Delta R}{dt} = k_a C(\Delta R_{max} - \Delta R) - k_d \Delta R \quad (2)$$

$$\text{Scatchard } \frac{\Delta R_{ex}}{[C]} = K_A \left(\Delta R_{max} - \Delta R_{eq}\right) \quad (3)$$

$$\text{Langmuir } \Delta R = \left\{\frac{\Delta R_{max}\,[C]}{K_D} + [C]\right\} \quad (4)$$

$$\text{Freundlich } \Delta R = DR_{max}\,[C]^{1/n} \quad (5)$$

$$\text{Langmuir–Freundlich } \Delta R = \left\{\frac{\Delta R_{max}\,[C]^{1/n}}{K_D} + [C]^{1/n}\right\} \quad (6)$$

%ΔR stands for the measured SPR signal response upon binding, and C for the BPA concentration. The forward and reverse equilibrium constants are denoted by K_A and K_D,

Preprints (www.preprints.org) | NOT PEER-REVIEWED | Posted: 19 December 2023 doi:10.20944/preprints202312.1431.v1

respectively. The forward and backward reactions' kinetic rate constants are denoted by the numbers ka and kd, respectively, while 1/n means the Freundlich exponent.

Figure 3A plots the ΔR values of the MIP-Au sensor against time for various BPA concentrations. Increasing BPA concentration causes a linear increase in the SPR response with high affinity for 0.1 to 10 ppb ($R^2 = 0.97$) the concentration range of BPA as shown in Figure 3B. Graph for the equilibrium binding is displayed also In Figure 3C.

The constants and values including ΔR_{max}, R^2, K_A, and K_D which are related with the kinetic studies were estimated to assess the adsorption dynamics of BPA and were given in Table 1. The most appropriate binding model was Langmuir isotherm which means BPA binds to the MIP-Au sensor in a monolayer according to the results. Table 2 represents the equilibrium binding isotherm parameters deduced from the graph lines shown in Figure 3D–F. The matrix effect was evaluated in BPA-spiked waste water because the presence of the residues in the analyzed sample affected the signal response and the linearity of the MIP-Au sensor response for the 0.2–10 ppb concentration range of BPA was also tested (R^2=0.98). It was found that the sample matrix had little to no impact on the MIP-Au sensor's sensitivity. This may be due to the absence of molecules similar in size and shape that present naturally in waste water and can cause a steric effect or act as a competing agent. In addition to a satisfactory linear regression constant being reported for waste water, a remarkable detection limit of 0.08 ng/L was also established.

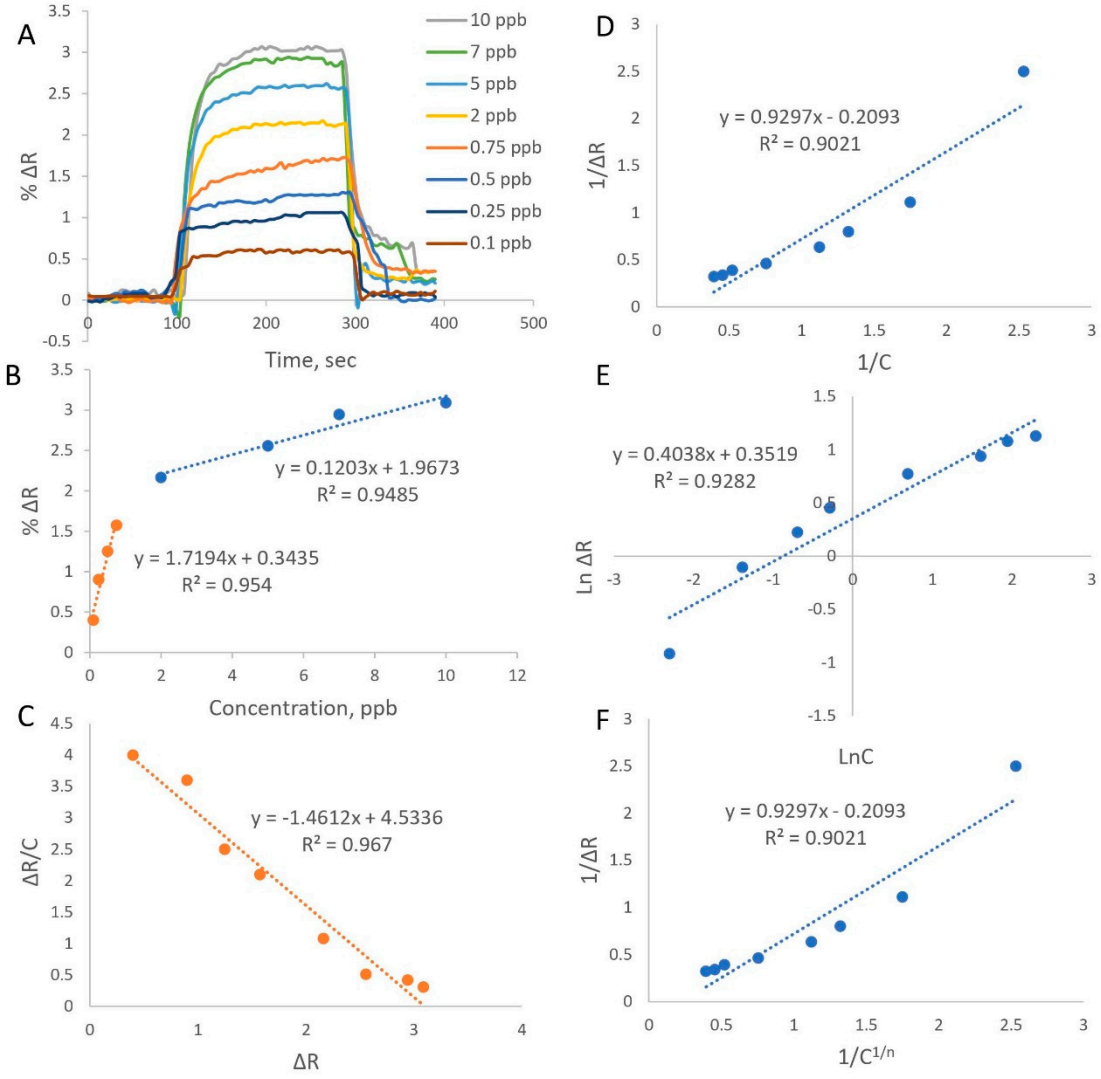

Figure 3. The assessment of kinetic parameters and adsorption isotherm models. A. MIP-Au sensor response graphs for the 0.1–10 ppb BPA concentration. B. MIP-Au sensor linear response for 0.1–10 ppb BPA concentration. C. Equilibrium binding analysis (Scatchard). D. Langmuir isotherm model E. Freundlich isotherm model F. Langmuir-Freundlich isotherm model.

 doi:10.20944/preprints202312.1431.v1

Table 1. Kinetic parameters.

Equilibrium analysis (Scatchard)		**Association kinetics analysis**	
ΔR_{max}	3.1	k_a, $(ng.mL^{-1})^{-1}.s^{-1}$	0.15
K_A, $(ng.mL^{-1})^{-1}$	1.46	k_d, s^{-1}	0.012
K_D, $ng.mL^{-1}$	0.68	K_A, $(ng.mL^{-1})^{-1}$	9.56
R^2	0.97	K_D, $ng.mL^{-1}$	0.10
		R^2	0.98

Table 2. Equilibrium binding isotherm parameters.

Langmuir		**Freundlich**		**Langmuir-Freundlich**	
ΔR_{max}	3.04	ΔR_{max}	1.42	ΔR_{max}	4.77
K_A, $(ng.mL^{-1})^{-1}$	14.13	1/n	0.40	K_A, $(ng.mL^{-1})^{-1}$	0.22
K_D, $ng.mL^{-1}$	0.07	R^2	0.92	K_D, $ng.mL^{-1}$	4.44
R^2	0.99			R^2	0.90

3.3. Determination of sensitivity, selectivity and imprinting efficiency

MIPs have imprinted sites used as recognition elements that resemble the template molecules in terms of their size and geometry. These imprinted sites function specifically and increase target molecule rebinding efficiency. The distribution and selectivity coefficients for 4-nitrophenol and phenol were determined using equation (7) as follows; Numbered lists can be added as follows:

$$Kd = [(C_i - C_e)/C_e]xV/m \quad (7)$$

The selectivity coefficient (k) was calculated using Equation 8.

$$k = K_{d\ template} / K_{d\ non\text{-}template} \quad (8)$$

The relative selectivity coefficient (k') was calculated using equation 9.

$$k' = k_{\Delta RMIP} / k_{\Delta RNIP} \quad (9)$$

K_d in equations refers to the distribution coefficient, whereas C_i and C_e represent the BPA molecule's starting and equilibrium concentrations. ΔR values were used as the relative selectivity coefficients in Equation 10, because of the unknown polymer amount (m). Additionally, many techniques have been created to improve the sensitivity of SPR biosensors and to quantify analytes at incredibly low concentrations. The majority of these techniques work by using various chemicals or nanoparticles that are caught by the sensor surface to alter the refractive index at the sensor surface. To bind the target analyte, main biorecognition elements are utilized. These techniques make use of dielectric or metallic nanoparticles, secondary and tertiary antibodies, enzyme-labeled antibodies, and secondary and tertiary antibodies [40,41]. To improve the responsiveness of SPR biosensors, gold spherical nanoparticles with a diameter of 5 to 40 nm have been employed extensively [42]. ΔR values for 10 ppb BPA applied to MIP-Au and MIP sensors showed that AuNPs improved signal responsiveness. By boosting the signal response for BPA detection, the AuNPs improved the MIP-Au sensor's sensitivity. Table 3 displays the signal response values for MIP-Au, NIP-Au, and MIP sensors.

Table 3. The selectivity and relative selectivity coefficient parameters of MIP, MIP-Au and NIP-Au SPR sensors.

	MIP		**MIP-Au**		**NIP-Au**		
	ΔR	**k**	**ΔR**	**k**	**ΔR**	**k**	**k'**
BPA	2.79	-	3.02	-	1.45	-	-
4-Nitrophenol	1.13	2.47	1.26	2.39	1.13	1.28	1.87
Phenol	1.35	2.06	1.5	2.01	1.15	1.26	1.60

Preprints (www.preprints.org) | NOT PEER-REVIEWED | Posted: 19 December 2023 doi:10.20944/preprints202312.1431.v1

In order to determine BPA selectively, competing adsorption studies were carried out in the presence of various structural analogues such as 4-nitrophenol, and phenol, respectively, Selectivity assessment for the target BPA molecule was conducted by applying competitor molecules to MIP-Au sensor and selectivity parameters were reported. The results are summarized in Table 3 along with the relative selectivity coefficient parameters. In comparison to competitor molecules 4-nitrophenol, and phenol, the MIP-Au sensor SPR nanosensor exhibited 2.47 and 2.06 times greater selectivity in detecting the target BPA molecule than the competing substances. The utilization of the molecular imprinting technique resulted in the formation of template-shaped cavities within polymer matrices, demonstrating predetermined selectivity and a strong affinity for the detection of BPA. In order to assess the imprinting efficiency of the MIP-Au sensor, the imprinting factor (I.F: 2.08) was determined by comparing the BPA signal response (ΔR values) produced by the MIP-Au sensor signal with the NIP-Au sensor, signal. Also, it was determined that the MIP-Au sensor was 1.87 times more selective for 4-nitrophenol and 1.60 times more selective for phenol when compared to the NIP-Au sensor for BPA based on the relative selectivity values of the two sensors (Figure 4). So, the MIP-Au sensor was verified to exhibit selective detection of the BPA molecule compared to 4-nitrophenol, and phenol, and it demonstrated more efficient BPA detection than the MIP-Au sensor. The low detection limit (LOD=10 ng/L) and good sensitivity and selectivity were demonstrated by the MIP-Au sensor utilized to detect BPA. LOD was estimated using the formula LOD = 3.3 (SD/S) based on the standard deviation of the response (SD) of the curve and the slope of the calibration curve (S) at values corresponding to the LOD.

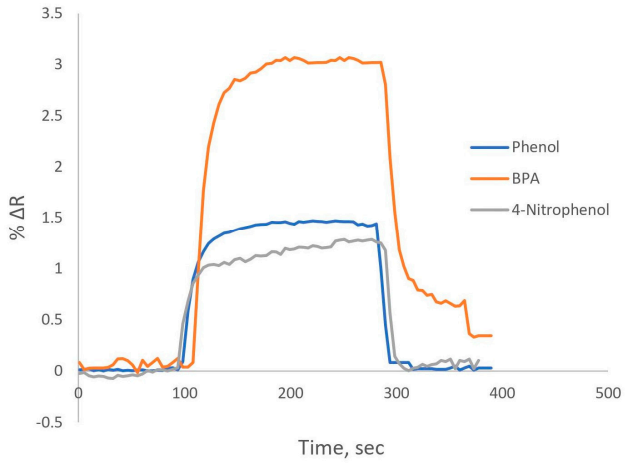

Figure 4. SPR sensorgrams showing the selectivity of MIP-Au sensor.

In comparison to an NIP-Au sensor made without a BPA molecule, the MIP-Au sensor's BPA imprinting effectiveness was calculated. Equation (1) was used to compute the imprinting factor in order to assess imprinting effectiveness. The MIP-Au sensor's ΔR value for BPA is 3.02, whereas the NIP-Au sensor's ΔR value is 1.45. The imprinting factor of 2.08 shows that imprinting was successfully accomplished.

3.4. Reusability and repeatability

The challenge in utilizing biological molecules as sensor recognition elements arises from their susceptibility to denaturation during the regeneration phase. Because of the durability of their polymeric structures, MIPs can withstand extreme environmental conditions. Studies on reproducibility were conducted using MIP-Au sensor system with four successive applications of a 10 ppb BPA solution (Figure 5). It was noted that the BPA detection capability was not changed noticeably.

Preprints (www.preprints.org) | NOT PEER-REVIEWED | Posted: 19 December 2023 doi:10.20944/preprints202312.1431.v1

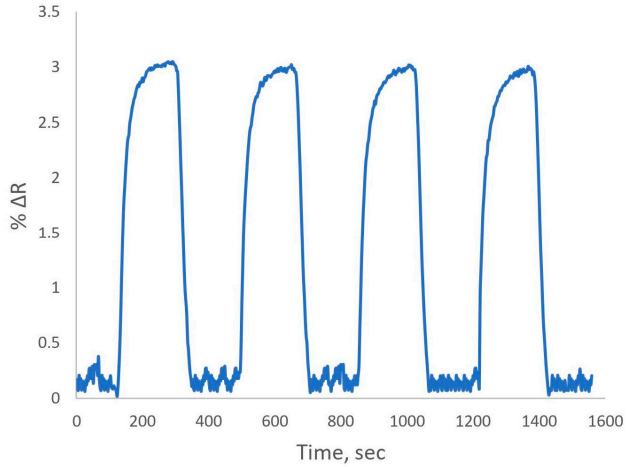

Figure 5. Reusability of MIP-Au sensor. BPA concentration: 10 ppb.

By incorporating a 10 ppb BPA solution and running it through the device four times, repeatability studies of the MIP-Au sensor system were assessed. A statistical analysis of the MIP-Au sensor's repeatability tests for 10 ppb BPA revealed a minimal decline in the detection of BPA after four adsorption-desorption cycles, as indicated by the percent relative standard deviation of the intraday assays of less than 1.25%.

4. Conclusion

Environmental pollutant detection and monitoring will always be difficult in various study domains. Pollutants, both well-known and undiscovered, are continuously introduced into the environment by growing waste production and new product development. Analytical sensors must thus always be developed and enhanced in order to monitor environmental pollutants. MIPs are durable, stable in aqueous and organic solvents, stable at severe pH values and temperatures, and they have a low-cost synthesis process in addition to offering selectivity. MIPs, which are extremely selective and sensitive to template molecules, are a relatively recent strategy in wastewater treatment and are excellent materials for this use. Therefore, especially when combined with plasmonic-based approaches, they are excellent candidates to acquire new applications in the field of safeguarding the environment. In this work, an optical-based sensor was created employing monomers based on amino acids and modified with AuNPs for the molecular imprinting method's selective measurement of BPA. For that, we synthesized BPA-imprinted nanofilm consisting of amino acid-based functional monomers to detect selectively BPA from synthetic wastewater sample. Through increasing the signal response for BPA detection, the AuNPs improved the MIP-Au sensor's sensitivity. It was found that the MIP-Au sensor was 1.60-fold selective for phenol and 1.87-fold selective for 4-nitrophenol. To assess the specificity of the MIP-Au sensor in detecting BPA, the imprinting efficiency was evaluated by comparing it with the non-imprinted MIP-Au sensor. The determined imprinting factor (I.F: 2.08) provides evidence that the MIP-Au sensor exhibits specific detection of BPA molecules. Considering the uniform distribution of binding sites, the Langmuir isotherm model provided the most accurate explanation for the interactions between the MIP-Au sensor and BPA. Due to the inherent stability of the polymeric structures in MIPs, they exhibit resistance to harsh environmental conditions. Repeatability testing involved subjecting the SPR system to four consecutive applications of a 10 ppb BPA solution. The findings indicated that the BPA detection capacity of the MIP-Au sensor, employed for BPA determination, did not experience a significant decrease, maintaining the repetition capacity of signal response (RSD < 1.5). The proposed BPA-imprinted SPR sensor offers high sensitivity based on the signal amplification technique using gold nanoparticles, unconjugated sensing without the need for labeling, real-time sensing, low sample consumption rates, quantifiable assessment, and excellent kinetic rate constant assessment in actual samples.

Author Contributions: Conceptualization, F.Y.; methodology, S.A.; software, D.T.; validation, D.T; formal analysis, I.G.; investigation, F.Y.; resources, I.G.; data curation, D.T.; writing—original draft preparation, I.G; writing—review and editing, S.A.; visualization, D.T.; supervision, A.D.; project administration A.D., All authors have read and agreed to the published version of the manuscript.

Funding: There are no funds to be declared.

Institutional Review Board Statement: Not applicable.

Data Availability Statement: Not applicable.

Acknowledgments: Not applicable.

Conflicts of Interest: The authors declare no conflict of interest.

References

1. Geens, T.; Goeyens, L.; Covaci, A. Are potential sources for human exposure to bisphenol-A overlooked? Int. J. Hyg. Environ. Health 2011, 214, 339–347, doi:10.1016/j.ijheh.2011.04.005.
2. Fasano, E.; Esposito, F.; Scognamiglio, G.; Di Francesco, F.; Montuori, P.; Amodio Cocchieri, R.; Cirillo, T. Bisphenol A contamination in soft drinks as a risk for children's health in Italy. Food Addit. Contam. - Part A Chem. Anal. Control. Expo. Risk Assess. 2015, 32, 1207–1214, doi:10.1080/19440049.2015.1031713.
3. Zoeller, R.T.; Bansal, R.; Parris, C. Bisphenol-A, an environmental contaminant that acts as a thyroid hormone receptor antagonist in vitro, increases serum thyroxine, and alters RC3/neurogranin expression in the developing rat brain. Endocrinology 2005, 146, 607–612, doi:10.1210/en.2004-1018.
4. Moriyama, K.; Tagami, T.; Akamizu, T.; Usui, T.; Saijo, M.; Kanamoto, N.; Hataya, Y.; Shimatsu, A.; Kuzuya, H.; Nakao, K. Thyroid hormone action is disrupted by bisphenol A as an antagonist. J. Clin. Endocrinol. Metab. 2002, 87, 5185–5190, doi:10.1210/jc.2002-020209.
5. Pelch, K.; Wignall, J.A.; Goldstone, A.E.; Ross, P.K.; Blain, R.B.; Shapiro, A.J.; Holmgren, S.D.; Hsieh, J.H.; Svoboda, D.; Auerbach, S.S.; et al. A scoping review of the health and toxicological activity of bisphenol A (BPA) structural analogues and functional alternatives. Toxicology 2019, 424, 152235, doi:10.1016/j.tox.2019.06.006.
6. Ma, Y.; Liu, H.; Wu, J.; Yuan, L.; Wang, Y.; Du, X.; Wang, R.; Marwa, P.W.; Petlulu, P.; Chen, X.; et al. The adverse health effects of bisphenol A and related toxicity mechanisms. Environ. Res. 2019, 176, doi:10.1016/j.envres.2019.108575.
7. Servos, M.R.; Bennie, D.T.; Burnison, B.K.; Jurkovic, A.; McInnis, R.; Neheli, T.; Schnell, A.; Seto, P.; Smyth, S.A.; Ternes, T.A. Distribution of estrogens, 17β-estradiol and estrone, in Canadian municipal wastewater treatment plants. Sci. Total Environ. 2005, 336, 155–170, doi:10.1016/j.scitotenv.2004.05.025.
8. Malekinejad, H.; Rezabakhsh, A. Hormones in dairy foods and their impact on public health- A narrative review article. Iran. J. Public Health 2015, 44, 742–758.
9. Wang, H.; Liu, Z. hua; Tang, Z.; Zhang, J.; Yin, H.; Dang, Z.; Wu, P. xiao; Liu, Y. Bisphenol Analogues in Chinese Bottled Water: Quantification and Potential Risk Analysis. *Sci. Total Environ.* **2020**, *713*, 136583, doi:10.1016/j.scitotenv.2020.136583.
10. Ashfaq, M.; Sun, Q.; Zhang, H.; Li, Y.; Wang, Y.; Li, M.; Lv, M.; Liao, X.; Yu, C.P. Occurrence and Fate of Bisphenol A Transformation Products, Bisphenol A Monomethyl Ether and Bisphenol A Dimethyl Ether, in Wastewater Treatment Plants and Surface Water. *J. Hazard. Mater.* **2018**, *357*, 401–407, doi:10.1016/j.jhazmat.2018.06.022.
11. Banaderakhshan, R.; Kemp, P.; Breul, L.; Steinbichl, P.; Hartmann, C.; Fürhacker, M. Bisphenol A and Its Alternatives in Austrian Thermal Paper Receipts, and the Migration from Reusable Plastic Drinking Bottles into Water and Artificial Saliva Using UHPLC-MS/MS. *Chemosphere* **2022**, *286*, 131842, doi:10.1016/j.chemosphere.2021.131842.
12. Jin, Z.; Zheng, W.; Liu, Y.; Xu, Z.; Zhao, Y. Facile Preparation of Electroactive Au@Ru Cups for Sensitive Detection of Bisphenol A. *ACS Sustain. Chem. Eng.* **2023**, *11*, 7673–7682, doi:10.1021/acssuschemeng.2c07570.
13. Wu, J.; Wei, W.; Zareef, M.; Li, S.; Ouyang, Q.; Chen, Q. Simple Design of Upconversion Nanoparticles-Based Aptasensor Integrated Microfluidic Chip for Ultra-Sensitive Detection of Bisphenol A in Aquatic Products. *Sensors Actuators B Chem.* **2023**, *390*, 134017, doi:10.1016/j.snb.2023.134017.
14. Sunil Kumar Naik, T.S.; Singh, S.; N, P.; Varshney, R.; Uppara, B.; Singh, J.; Khan, N.A.; Singh, L.; Zulqarnain Arshad, M.; C. Ramamurthy, P. Advanced Experimental Techniques for the Sensitive Detection of a Toxic Bisphenol A Using UiO-66-NDC/GO-Based Electrochemical Sensor. *Chemosphere* **2023**, *311*, 137104, doi:10.1016/j.chemosphere.2022.137104.
15. Zhu, Y.P.; Yang, L.; Wang, A.J.; Feng, J.J. Graphitic Carbon-Coated PtCoNi Alloys Supported on N-Doped Porous Carbon Nanoflakes for Sensitive Detection of Bisphenol A. *ACS Appl. Nano Mater.* **2023**, *6*, 8726–8734, doi:10.1021/acsanm.3c01113.

16. Liu, Y.H.; Liu, C.; Wang, X.H.; Li, T.; Zhang, X. Electrochemical Sensor for Sensitive Detection of Bisphenol A Based on Molecularly Imprinted TiO2 with Oxygen Vacancy. *Biosens. Bioelectron.* **2023**, *237*, 115520, doi:10.1016/j.bios.2023.115520.
17. El Hani, O.; Karrat, A.; Digua, K.; Amine, A. Advanced Molecularly Imprinted Polymer-Based Paper Analytical Device for Selective and Sensitive Detection of Bisphenol-A in Water Samples. Microchem. J. 2023, 184, 108157, doi:10.1016/j.microc.2022.108157.
18. Xue, J.Q.; Li, D.W.; Qu, L.L.; Long, Y.T. Surface-imprinted core-shell Au nanoparticles for selective detection of bisphenol A based on surface-enhanced Raman scattering. Anal. Chim. Acta 2013, 777, 57–62, doi:10.1016/j.aca.2013.03.037.
19. Uchida, A.; Kitayama, Y.; Takano, E.; Ooya, T.; Takeuchi, T. Supraparticles comprised of molecularly imprinted nanoparticles and modified gold nanoparticles as a nanosensor platform. RSC Adv. 2013, 3, 25306–25311, doi:10.1039/c3ra43660h.
20. Wang, Z.; Yan, R.; Liao, S.; Miao, Y.; Zhang, B.; Wang, F.; Yang, H. In situ reduced silver nanoparticles embedded molecularly imprinted reusable sensor for selective and sensitive SERS detection of Bisphenol A. Appl. Surf. Sci. 2018, 457, 323–331, doi:10.1016/j.apsusc.2018.06.283.
21. Zhu, C.; Zhang, L.; Chen, C.; Zhou, J. Determination of Bisphenol A using a Molecularly Imprinted Polymer Surface Plasmon Resonance Sensor. Anal. Lett. 2015, 48, 1537–1550, doi:10.1080/00032719.2014.996809.
22. Lazarević-Pašti, T.; Tasić, T.; Milanković, V.; Potkonjak, N. Molecularly Imprinted Plasmonic-Based Sensors for Environmental Contaminants—Current State and Future Perspectives. Chemosensors 2023, 11, doi:10.3390/chemosensors11010035.
23. Gokturk, I.; Bakhshpour, M.; Cimen, D.; Yilmaz, F.; Bereli, N.; Denizli, A. SPR Signal Enhancement With Silver Nanoparticle-Assisted Plasmonic Sensor for Selective Adenosine Detection. IEEE Sens. J. 2022, 22, 14862–14869, doi:10.1109/JSEN.2022.3186518.
24. Shama, N.A.; Aşır, S.; Göktürk, I.; Yılmaz, F.; Türkmen, D.; Denizli, A. Electrochemical Detection of Cortisol by Silver Nanoparticle-Modified Molecularly Imprinted Polymer-Coated Pencil Graphite Electrodes. ACS Omega 2023, 8, 29202–29212, doi:10.1021/acsomega.3c02472.
25. Derazshamshir, A.; Göktürk, I.; Tamahkar, E.; Yılmaz, F.; Sağlam, N.; Denizli, A. Phenol removal from wastewater by surface imprinted bacterial cellulose nanofibres. Environ. Technol. (United Kingdom) 2020, 41, 3134–3145, doi:10.1080/09593330.2019.1600043.
26. Shama, N.A.; Aşır, S.; Ozsoz, M.; Göktürk, I.; Türkmen, D.; Yılmaz, F.; Denizli, A. Gold-Modified Molecularly Imprinted N-Methacryloyl-(L)-phenylalanine-containing Electrodes for Electrochemical Detection of Dopamine. Bioengineering 2022, 9, doi:10.3390/bioengineering9030087.
27. Türkmen, D.; Bakhshpour, M.; Göktürk, I.; Aşir, S.; Yilmaz, F.; Denizli, A. Selective dopamine detection by SPR sensor signal amplification using gold nanoparticles. New J. Chem. 2021, 45, 18296–18306, doi:10.1039/d1nj01938d.
28. Bakhshpour, M.; Göktürk, I.; Bereli, N.; Yılmaz, F.; Denizli, A. Selective detection of penicillin g antibiotic in milk by molecularly imprinted polymer-based plasmonic spr sensor. Biomimetics 2021, 6, doi:10.3390/biomimetics6040072.
29. Wang, Y.; Niu, Z.; Xu, C.; Zhan, M.; Koh, K.; Niu, J.; Chen, H. 2D MOF-Enhanced SPR Sensing Platform : Facile and Ultrasensitive Detection of Sulfamethazine via Supramolecular Probe. J. Hazard. Mater. 2023, 456, 131642, doi:10.1016/j.jhazmat.2023.131642.
30. Karki, B.; Hma, N.; Gaurav, S.; Arjuna, S.; Ram, M.; Yadav, B. A Simulation Study for Dengue Virus Detection Using Surface Plasmon Resonance Sensor Heterostructure of Silver , Barium Titanate , and Cerium Oxide. Plasmonics 2023, 2031–2040, doi:10.1007/s11468-023-01907-9.
31. Karki, B.; Uniyal, A.; Sarkar, P.; Pal, A. Sensitivity Improvement of Surface Plasmon Resonance Sensor for Glucose Detection in Urine Samples Using Heterogeneous Layers : An Analytical Perspective. J. Opt. 2023, doi:10.1007/s12596-023-01418-0.
32. Jiang, T.; Ye, X.; Ge, L.; Guo, H.; Sassa, F.; Hayashi, K. Chemical and Biological Sensors Subpixel Patterned LSPR Gas Sensor Array With Using Inkjet Printing Au / Ag Nanoparticle to Enhance the Selectivity. IEEE Sensors Lett. 2023, 7, 1–4, doi:10.1109/LSENS.2023.3300820.
33. Singh, L.; Vasimalla, Y.; Kumar, R.; Pareek, P. Optik Highly Sensitive Surface Plasmon Resonance Sensor for Refractive Index Detection of Helicobacter Pylori. Optik (Stuttg). 2023, 274, 170516, doi:10.1016/j.ijleo.2023.170516.
34. Gomaa, M.; Salah, A.; Abdel, G. Superior Enhancement of SPR Fiber Optic Sensor Using Laser Sensitized Dip-Coated Graphene Gold Nanocomposite Probes. Opt. Laser Technol. 2023, 157, 108644, doi:10.1016/j.optlastec.2022.108644.
35. Sharma, V.; Kumar, A.; Saharan, S.; Semwal, S. Graphene / Au / MIP - Coated D - Shaped Optical Fiber – Based SPR Sensor for Ethanol Detection. Plasmonics 2023, 1639–1649, doi:10.1007/s11468-023-01920-y.
36. Hix-janssens, T.; Shinde, S.; Abouhany, R.; Davies, J.; Neilands, J. Microcontact-Imprinted Optical Sensors for Virulence Factors of Periodontal Disease. 2023, 1–19.

37. Skeletal-, D.; Analytes, C. Molecularly Imprinted Polymer-Based Sensors for the Detection of Skeletal- and Cardiac-Muscle-Related Analytes. 2023.
38. Bashar, F.; Eddin, K.; Wing, Y.; Ying, J.; Liew, C. Development of Plasmonic-Based Sensor for Highly Sensitive and Selective Detection of Dopamine. Opt. Laser Technol. 2023, 161, 109221, doi:10.1016/j.optlastec.2023.109221.
39. Uzun, L.; Türkmen, D.; Yilmaz, E.; Bektaş, S.; Denizli, A. Cysteine functionalized poly(hydroxyethyl methacrylate) monolith for heavy metal removal. Colloids Surfaces A Physicochem. Eng. Asp. 2008, 330, 161–167, doi:10.1016/j.colsurfa.2008.07.045.
40. Chaudhary, V.S.; Kumar, D.; Kumar, S. Gold-Immobilized Photonic Crystal Fiber-Based SPR Biosensor for Detection of Malaria Disease in Human Body. IEEE Sens. J. 2021, 21, 17800–17807, doi:10.1109/JSEN.2021.3085829.
41. Chaudhary, V.S.; Kumar, D.; Mishra, G.P.; Sharma, S.; Kumar, S. Plasmonic Biosensor With Gold and Titanium Dioxide Immobilized on Photonic Crystal Fiber for Blood Composition Detection. IEEE Sens. J. 2022, 22, 8474–8481, doi:10.1109/JSEN.2022.3160482.
42. Špringer, T.; Ermini, M.L.; Špačková, B.; Jabloňků, J.; Homola, J. Enhancing sensitivity of surface plasmon resonance biosensors by functionalized gold nanoparticles: Size matters. Anal. Chem. 2014, 86, 10350–10356, doi:10.1021/ac502637u.